



The scaffold protein, Homer1b/c, regulates axon pathfinding in the central nervous system *in vivo*

Lisa Foa¹, Indrani Rajan¹, Kurt Haas¹, Gang-Yi Wu¹, Paul Brakeman², Paul Worley² and Hollis Cline¹

¹ Cold Spring Harbor Laboratory, Beckman Building, 1 Bungtown Road, Cold Spring Harbor, New York 11724, USA

² Department of Neuroscience, Johns Hopkins University School of Medicine, Baltimore, Maryland 21205, USA

The first two authors contributed equally to this work

Correspondence should be addressed to H.C. (cline@cshl.org)

Homer proteins are a family of multidomain cytosolic proteins that have been postulated to serve as scaffold proteins that affect responses to extracellular signals by regulating protein–protein interactions. We tested whether Homer proteins are involved in axon pathfinding *in vivo*, by expressing both wild-type and mutant isoforms of Homer in *Xenopus* optic tectal neurons. Time-lapse imaging demonstrated that interfering with the ability of endogenous Homer to form protein–protein interactions resulted in axon pathfinding errors at stereotypical choice points. These data demonstrate a function for scaffold proteins such as Homer in axon guidance. Homer may facilitate signal transduction from cell-surface receptors to intracellular proteins that govern the establishment of axon trajectories.

Axon pathfinding during early stages of CNS development is essential to establish the fundamental connectivity of the brain. Mechanisms of axon pathfinding include receptor-mediated recognition of attractive and repulsive cues in the environment, which induce changes in the direction of the axonal growth cone. Alterations in growth cone behavior in response to environmental cues require cytoskeletal rearrangements; however, the cellular components that transduce signals from cell surface receptors to the cytoskeleton remain elusive^{1,2}. Receptor-mediated regulation of growth cone motility requires a complex of proteins including transmembrane or membrane-bound receptors, signaling proteins, scaffold proteins and cytoskeletal components^{1–3}. Multivalent binding proteins can form scaffolds to anchor proteins and regulate their function within multiprotein signaling complexes^{4–6}. Despite considerable information concerning both the role of intracellular calcium^{7–10} and cytoskeletal dynamics^{3,11} in these events, little is known of the identity or function of scaffold proteins controlling growth cone behavior.

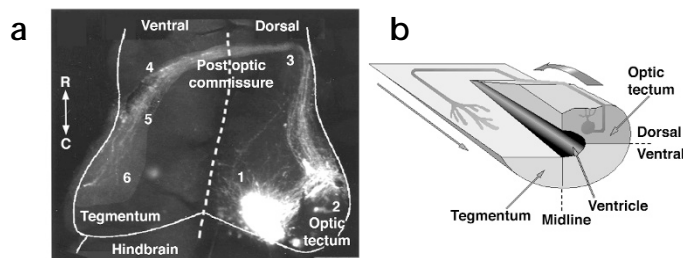
The Homer family of proteins¹² (also called vesl (ref. 13), CPG22 (ref. 14), PSD-zip45 (ref. 15) and Cupidin¹⁶) have been postulated to act as cytosolic scaffold proteins, possibly linking cell surface transmembrane receptors and intracellular calcium stores^{17–19} or regulating transmembrane receptor trafficking and anchoring^{20–24}. Homer proteins are derived from three genes in mammals and one gene in *Drosophila*¹⁷. Each gene in mammals can generate alternately spliced isoforms. Homer proteins are highly conserved across species and are characterized by an enabled VASP homology (EVH1) domain encoded by the N-terminal 112 amino acids of all Homer proteins. One form of Homer, Homer1a, is induced in response to neuronal activity in rodents^{12,13,15} and *Xenopus* (unpublished data). Homer1a encodes a truncated form of the other Homer isoforms, consist-

ing of the EVH1 domain. The expression of all other forms of Homer is not affected by activity^{13,17}. The constitutively expressed Homer proteins contain the EVH1 domain and a C-terminal coiled-coil (CC) domain^{4,17,18,23}, and will be called the long forms of Homer. The long forms of Homer multimerize through association of their CC domains. The Homer dimers then have the capacity to crosslink multiple interacting proteins through their ligand-binding EVH1 domains. The EVH1 domain of Homer1a binds to the same proteins as the long forms of Homer; however, Homer1a cannot crosslink associated proteins because it lacks the CC domain.

Homer can associate with a variety of proteins, including transmembrane receptors such as class 1 metabotropic glutamate receptors (mGluRs), inositol triphosphate receptors (IP₃R), ryanodine receptors (RyR)^{12,18,23} and other anchoring proteins such as Shank¹⁹. All the known protein–protein interactions between Homer proteins and their binding partners are due to the EVH1 domain binding a conserved proline-rich motif in the ligands²⁵. Although Homer proteins are characterized by their EVH1 domain, Homer does not bind ligands of other EVH1 proteins, such as Ena, VASP or WASP, because of a unique structure of the binding pocket in the Homer EVH1 domain²⁵.

We tested whether Homer proteins are involved in axon pathfinding via their ability to crosslink interacting proteins that govern growth cone behaviors. We expressed both long and short forms of Homer, as well as mutant Homer proteins that do not bind ligands. We assessed the effect of expression of the different Homer proteins on axon pathfinding *in vivo* by collecting time-lapse images of optic tectal cell axonal projections in *Xenopus* tadpoles over periods of 3–5 days. The data indicate that full-length Homer proteins are essential for axon pathfinding *in vivo*. The data support the hypothesis that Homer proteins act as scaffold

Fig. 1. Axon trajectory of optic tectal neurons. (a) Biocytin-labeled cluster of optic tectal neurons reveals their projection patterns. Confocal images collected through the z-axis of the midbrain region. The right half of the image shows a stack of confocal images collected through the dorsal part of the midbrain. The left half is a stack of confocal images collected through the ventral part of the midbrain. Axons navigate six choice points as they extend to the target. (1) As soon as the axon extends from the soma of a newly differentiated neuron, it makes the first choice to grow toward lateral or medial tectum. Most tectal axons extend laterally within the tectal neuropil, whereas a fraction of the cells extend an axon toward the medial edge of the tectum. These axons avoid the dorsal midline and extend rostrally within the medial tract of the same tectal lobe. (2) Axons turn rostrally or caudally. (3) Rostrally projecting axons descend to the ventral aspect of the brain where they confront the third choice point, the postoptic commissure. Axons enter the commissure and cross to the contralateral side of the brain. (4) Axons exit the commissure and turn caudally. (5) Axons leave the ventral axon fascicle and grow slightly dorsally into the tegmentum. (6) Axons recognize tegmentum as target and establish a complex axonal arbor. (b) Axon trajectory of a rostrally projecting tectal cell. R, rostral; C, caudal. Scale bar, 100 μ m.



fold linking cell surface receptors to intracellular signaling pathways controlling axon pathfinding.

RESULTS

Tectal cell axonal projections

We used biocytin and DiI labeling of large clusters of optic tectal neurons to determine the normal axonal projection pattern. Rostrally projecting tectal axons navigate six choice points along a stereotyped pathway to their target in the contralateral tegmentum in the floor of the midbrain (Fig. 1). In Fig. 3 and subsequent figures, axons are labeled by the number of the choice point corresponding to the pathfinding error they make.

Expression of Homer isoforms in optic tectum

We cloned the *Xenopus* homolog of Homer1 from a tadpole brain library. The deduced amino acid sequence of the open reading frame of *Xenopus* Homer is highly homologous to murine Homer¹⁷. The N-terminal half of the *Xenopus* protein, including the EVH1 domain, through which Homer binds to other proteins, is 98% identical to the N-terminal of human Homer1.

Homer1b/c is expressed in *Xenopus* tadpole brain and is distributed throughout the optic tectum, including within newly differentiated neurons close to the caudomedial proliferative zone of the tectum (Fig. 2b and c). Neurons in this position within the tectum are in the process of extending their axons out of the tectum²⁶. Homer1b/c is located in a punctate pattern in tectal axonal growth cones (Fig. 2d and e). Homer1a is barely detectable in brain homogenates (Fig. 2b).

Homer regulates tectal cell axonal pathfinding

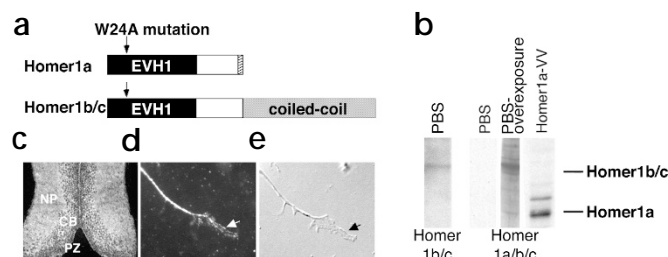
We investigated the function of Homer proteins in axon pathfinding of the rostrally projecting tectal neurons. We predicted that

expressing Homer1a would interfere with protein interactions required for signaling events governing axon guidance. We expressed Homer1a in optic tectal cells using either viral gene transfer or targeted electroporation. We injected vaccinia virus (VV) encoding Homer1a (Homer1a-VV) into the brain ventricle of stage 44/45 *Xenopus* tadpoles. Control stage-matched tadpoles were either uninfected or infected with a virus expressing the reporter β -galactosidase (β -gal-VV). Homer1a-VV-infected animals have higher Homer1a expression in tectal neurons compared to uninfected control animals (Fig. 2b) or animals infected with β -gal-VV (data not shown).

The axon trajectories of optic tectal neurons in VV-infected animals were determined by imaging localized clusters of DiI-labeled neurons over three days, starting two days after virus injection. Animals infected with β -gal-VV had axonal projections comparable to those of uninfected control animals (Fig. 3a and b). Labeling a large population of neurons in one tectal lobe revealed an occasional axon crossing the dorsal midline in 28.5% of uninfected and 29% of β -gal-VV-infected animals (Figs. 3a, b and 6a). Axons that cross the dorsal midline in either uninfected animals or β -gal-VV-infected animals were not observed in images taken 24 hours later (Fig. 3a and b), indicating that these aberrant projections were transient.

Animals infected with Homer1a-VV show persistent aberrant axon projections to the contralateral optic tectum (Fig. 3c). In the example in Fig. 3, a cluster of labeled tectal neurons (lower right corner of the image) projects a bundle of axons across the tectal midline on the first day of imaging. These neurons are located caudally in the optic tectum and demonstrate the midline crossing error seen in neurons that express Homer1a when they are first extending their axons. More rostrally positioned neurons, which are more mature, had already projected axons past the midline choice point when they were labeled with dye. These axons

Fig. 2. Homer isoforms are differentially expressed in *Xenopus* brain. (a) Homer1 isoforms. (b) Western blots showing Homer expression in tissue homogenates using two Homer antibodies. The Homer1b/c antibody recognizes the coiled-coil domain of Homer1b/c. The Homer1a/b/c antibody recognizes all forms of Homer1. Homer1a expression is increased after infection with Homer1a-VV compared to animals injected with PBS. Overexposure of the blot (PBS overexposure) shows Homer1b/c and very low levels of endogenous Homer1a. (c) Confocal image of the tadpole midbrain labeled with the Homer 1b/c antibody. Homer1b/c is concentrated in tectal cell bodies and the tectal neuropil. Rostral is up. (d, e) Homer1b/c is distributed in a granular pattern in tectal cell axonal growth cones (arrows, in fluorescence (d) and DIC (e) images). Scale bars (c), 100 μ m; (d, e), 10 μ m. PZ, proliferative zone; CB, tectal cell body region; NP, tectal neuropil.



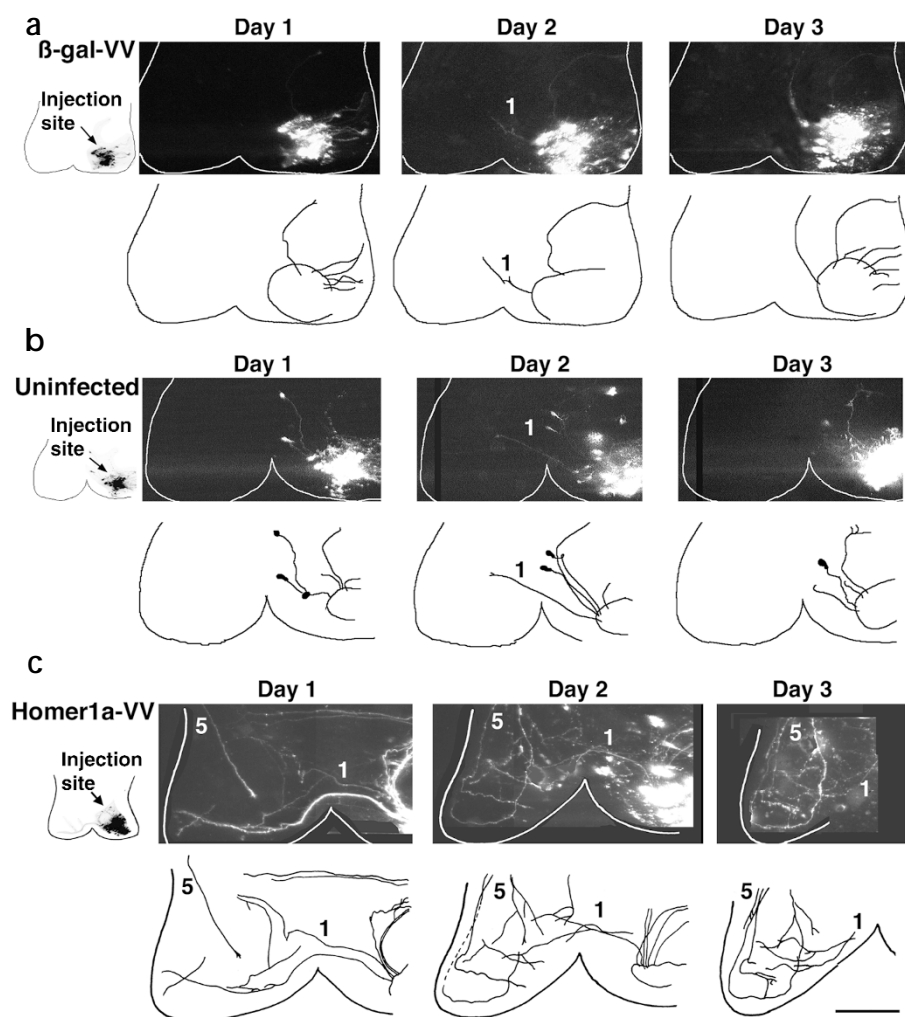


Fig. 3. Viral expression of Homer1a causes axon pathfinding errors. Time-lapse confocal images collected at 24-h intervals over 3 days showing Dil-labeled tectal cell axon projections to the contralateral optic tecta in representative β -gal-VV-infected (a), uninfected (b) and Homer1a-VV-infected (c) animals. Low-magnification images of the Dil injection site within an outline of the midbrain are shown to the left of each series. Drawings of the confocal image stacks are shown below each image. Numbers 1 and 5 refer to the type of axon projection errors. Scale bar, 100 μ m.

not expected to cause axon pathfinding errors, because it cannot bind Homer ligands.

Control cells expressing GFP project axons to the contralateral tegmentum, as seen with biocytin and Dil-labeled neurons (Fig. 4a–c). Electroporation of Homer1a caused the same types of axon pathfinding errors seen after viral expression of Homer1a (Figs. 4d–f and 6c–f). In addition, the superior imaging quality afforded by GFP allowed us to observe that some axons that make an error at the dorso-ventral choice point remain in the lateral tract and extend into the hindbrain (Fig. 6e and f). Homer1a expression also causes target recognition errors: axons enter the tegmental neuropil, but fail to arborize. Instead, they extend dorsally into the optic tectum

(#6 in Fig. 4d–f). Electroporation of the ligand-binding mutant of Homer1a, Homer1aW24A, does not cause pathfinding errors (Figs. 4g–i and 6c–e).

Homer1b/c functions in axon pathfinding

Homer dimers are thought to couple two Homer binding proteins within the scaffold complex. Expression of Homer1a is postulated to interfere with Homer function by displacing Homer1b/c from its ligands. The studies outlined above used Homer1a expression to interfere with endogenous Homer1b/c function. In the following experiments, we directly tested Homer1b/c function in axon guidance by introducing wild-type Homer1c or the mutant Homer1cW24A into a single tectal lobe by targeted electroporation. Homer1cW24A, which carries the same point mutation as Homer1aW24A, can dimerize with endogenous Homer1b/c via the CC domain, but does not bind Homer ligands. This construct is predicted to interfere with Homer function and cause axon projection errors. Overexpression of Homer1c alters calcium signaling through associated receptors²⁴, which suggests that specific levels of Homer1b/c are important for its function. Therefore, overexpression of Homer1c itself might also be predicted to affect axon pathfinding.

Overexpression of Homer1c or expression of Homer1cW24A causes the same axon pathfinding and target recognition errors as seen with expression of Homer1a (Fig. 4j–o). Tectal cells expressing

exit the tectum and cross to the contralateral side of the brain in the postoptic commissure on the floor of the midbrain. On the first day of imaging, a single axon tipped with a growth cone entered the left tectum rostrally (#5, Fig. 3c). Images collected through the z-axis of the brain show that this axon extended from the cluster of labeled tectal neurons in the right optic tectum, correctly navigated into the postoptic commissure, but then erroneously projected to the contralateral optic tectum, dorsal to the normal terminal field in tegmentum. Images collected from the same animal on the subsequent two days revealed additional axons that aberrantly entered the contralateral optic tectum, after making an error at choice point 5. These aberrant projections become more prevalent with longer times after infection with the Homer1a-VV. This likely reflects the time course of axon outgrowth from the infected neurons, because it takes 2–3 days for tectal cell axons to reach the contralateral tegmentum.

To further examine the function of Homer proteins in axon pathfinding, we used targeted electroporation to confine Homer1a expression to one tectal lobe. Electroporation of GFP fusion proteins of Homer1a, Homer1c and Homer1cW24A indicates that they are expressed throughout neurons, including throughout the axonal growth cones (data not shown). We compared the axon pathfinding of the Homer1a-expressing neurons to that of neurons expressing a point mutant that does not bind Homer ligands, Homer1aW24A²⁵. Expression of the mutant Homer1aW24A was

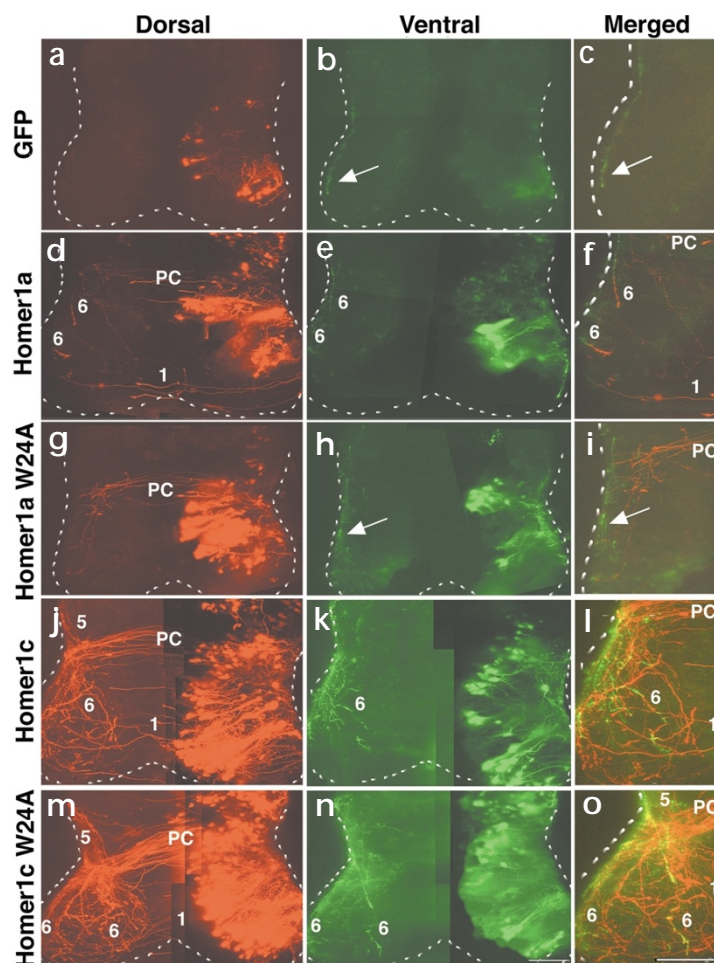


Fig. 4. Electroporation of Homer proteins causes axon pathfinding and target recognition errors. Confocal images collected through the midbrain, five days after either electroporation with GFP alone or co-electroporation of GFP with Homer constructs. In each case, the complete z-series was split into dorsal (pseudo-colored red) and ventral (pseudo-colored green) stacks. The merged image (right) is enlarged to illustrate the complete tectal axon trajectory through the contralateral tectum and tegmentum. (**a–c**) Whole-brain electroporation with GFP illustrates the normal trajectory of tectal axons. Tectal cells and dendrites are located in the dorsal tectum (**a**). Tectal cell axons terminating correctly in the contralateral tegmentum are marked by arrows (**b, c**). (**d–f**) Co-electroporation of GFP with Homer1a caused axon pathfinding errors at the dorsal midline (1) and at the dorsoventral choice point (data not shown). Homer1a expression also caused target recognition errors (6). The merged image in (**f**) shows single axons changing color from green to red, indicating that they aberrantly extended from ventral to dorsal sections. (**g–i**) Co-electroporation of the ligand-binding mutant Homer1aW24A and GFP results in tectal cell axons terminating correctly in the contralateral tegmentum (arrows). (**j–l**) Overexpression of Homer1c caused target recognition errors (6), and pathfinding errors at the dorsal midline (1) and the dorsoventral choice point (5). (**m–o**) Expression of the ligand-binding mutant Homer1cW24A caused axon pathfinding and target recognition errors at positions 1, 5 and 6. In all examples, thalamic axons that normally cross to the contralateral side of the brain via the posterior commissure are labeled PC. The dashed white outline of the brain was traced from transmitted light images. Scale bar, 100 μ m.

Homer1c or Homer1cW24A extend aberrant axon projections across the dorsal tectal midline (#1 in Fig. 4j, l, m and o). Axons also make errors at choice point 5 in the floor of the brain contralateral to the electroporated tectum (#5, Fig. 4j–o) and make target recognition errors in the contralateral tegmentum (#6 Fig. 4j–o). These data using electroporation of Homer constructs indicate that Homer functions cell autonomously to affect axon pathfinding.

Single-cell analysis of axon pathfinding errors

The above experiments suggest that the pathfinding error at the dorsal midline is made by younger neurons, which are just extending the axon from the cell body. The later contralateral pathfinding error is made by more mature neurons, which had already extended an axon past the midline choice point at the time we induced Homer1a expression. To test this further, we imaged single tectal neurons at different positions along the rostrocaudal axis of the developing tectum²⁶ in control and Homer1a-VV-infected animals. Single neurons were labeled either with DiI or by electroporation with GFP²⁷. Two-photon images of a single GFP-expressing neuron show a control axon projection to the contralateral tegmentum (Fig. 5a–c).

We collected time-lapse images over 24 hours from a relatively young DiI-labeled neuron in a Homer1a-VV-infected animal (Fig. 5d–f). At the first imaging session, the axon had grown across the dorsal tectal midline. By the next day, the errant projection looped back across the midline to the tectum from which it originated. More mature neurons had already extended an axon rostrally out of the tectum on the first day of imaging. Axons from

these neurons correctly navigated until the dorsoventral choice point, where they erroneously projected dorsally to the contralateral optic tectum (Fig. 5h, i, k and l).

Axons that project to the contralateral optic tectum can make yet another error, and cross the dorsal tectal midline to terminate in the tectal lobe containing the cell body from

which they originated (Fig. 5j–l). This indicates that Homer1a expression can cause axon errors at the tectal midline either early in the trajectory (as in the example in Fig. 5d–f) or later in the trajectory (Fig. 5j–l), when growth cones would never normally confront the dorsal midline.

Quantification of axon pathfinding errors

Comparable numbers of control (uninfected, β -gal-VV-infected or GFP-expressing) animals had axons that projected across the dorsal midline at each day of imaging (Fig. 6a and c). This indicates that viral infection or electroporation did not cause axon projection errors. Significantly more (χ^2 , $p < 0.05$) Homer1a-expressing animals had axons crossing the dorsal midline on all three days of imaging (Fig. 6a and c). For example, in the Homer1a-electroporated animals, the error rate was 56% on day 1 and increased to 88% on day 3, significantly greater values than for the control GFP-expressing animals (χ^2 , $p < 0.001$). These values underestimate the fraction of animals with axon pathfinding errors, because animals that did not exhibit dorsal midline errors did exhibit errors at the dorso-ventral choice point. Furthermore, when axons crossing the tectal midline were observed in the control animals, they were single axons per animal, whereas Homer1a-expressing animals typically had multiple errant axons (Figs. 3 and 4).

Homer1cW24A seems to act as a dominant negative by increasing the rate of dorsal midline errors. On the first day of imaging, 50% of Homer1cW24A-expressing animals had mid-

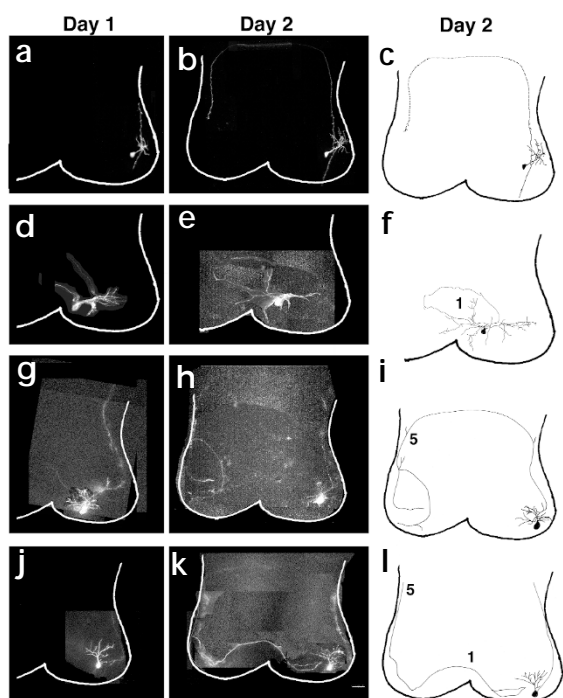


Fig. 5. Time-lapse analysis of axon projections in single tectal cells after Homer1a-VV infection. (a, b) Two-photon images of a single tectal neuron expressing GFP, collected at 24 h intervals, marked day 1 and day 2. (c) Drawing of the neuron at day 2 shows the normal tectal axon trajectory. The dashed line represents the ventral portion of the axon. (d-l) Single DiI-labeled tectal cell axon trajectories in three Homer1a-VV-infected animals. Each row shows a rendered stack of confocal images collected at daily intervals and a drawing of the neuron at day 2. Tectal cells in Homer1a-VV-infected animals make errors at the dorsal tectal midline (1) and at the dorsoventral choice point (5). Scale bar, 50 μ m.

line errors, significantly more errors than in the GFP controls (χ^2 , $p < 0.001$, Fig. 6c). The error rate remained significantly greater than controls throughout the imaging period. Overexpression of Homer1c increased midline error rates from 25% to 62% over the three days of imaging, also significantly greater than controls (χ^2 , $p < 0.001$, Fig. 6c).

Expression of both Homer1a and Homer1cW24A significantly increased the relative numbers of animals with aberrant projections to the contralateral optic tectum (Fig. 6d). For both con-

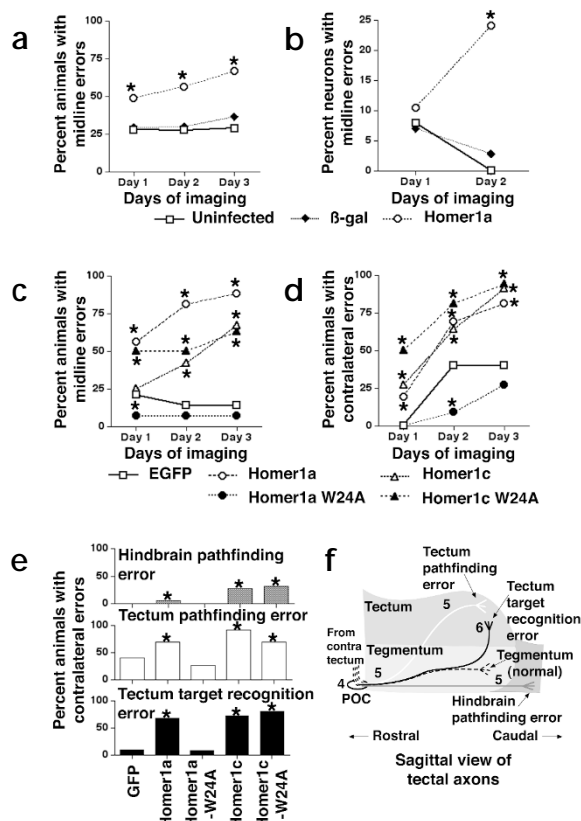
structs, the contralateral error rate was significantly greater than controls on the first day of imaging, and increased further over the next two days. Overexpression of Homer1c also led to increased numbers of animals with axons erroneously projecting to the contralateral tectum. Homer1aW24A did not cause errant projections to the contralateral optic tectum.

Homer1a, Homer1c and Homer1cW24A increased the frequency of each of the three error types analyzed, whereas Homer1aW24A did not increase the rate of these errors (Fig. 6e and f). This analysis suggests that Homer proteins function at each of these choice points.

Homer functions in axon error correction

Analysis of single DiI-labeled cells in Homer1a-VV-infected animals allowed a more accurate assessment of the effect of Homer1a expression on the frequency of axons crossing the dorsal tectal midline (Fig. 6b). In β -gal-VV-infected animals, the fraction of DiI-labeled neurons that extended an axon across the tectal midline decreased from 6% to 3% over 24 hours, comparable to the values from uninfected animals. In contrast, the fraction of

Fig. 6. Quantitative analysis of pathfinding and target recognition errors after Homer expression. (a) The percentage of animals with tectal cell axons crossing the dorsal midline was increased in Homer1a-VV-infected animals compared to uninfected and β -gal-VV-infected animals. Numbers of animals with midline errors on Days 1, 2 and 3 of imaging: uninfected, 10/35, 9/33, 9/33; β -gal-VV, 19/65, 17/58, 12/33; Homer1a-VV, 19/39, 22/39, 12/18. (b) Homer1a expression increases the percentage of single neurons with axons crossing the dorsal midline. Numbers of neurons with midline errors on Days 1 and 2 of imaging: uninfected, 2/25, 0/25; β -gal-VV, 3/48, 1/36; Homer1a-VV, 8/76, 14/58. (c) The percentage of animals with tectal cell axons crossing the dorsal midline consistently increased after Homer1a, Homer1c or Homer1cW24A electroporation. Numbers of animals with midline errors on Days 1, 2 and 3 of imaging: GFP, 3/14, 2/14, 2/14; Homer1a, 9/16, 13/16, 14/16; Homer1a W24A, 1/14, 1/14, 1/14; Homer1c, 3/12, 5/12, 8/12; Homer1c W24A, 8/16, 8/16, 10/16. (d) The percentage of animals with tectal axons making contralateral errors (pathfinding and target recognition errors combined) consistently increased after Homer1a, Homer1c or Homer1cW24A expression. Numbers of animals with contralateral errors on Days 1, 2 and 3 of imaging: GFP, 0/10, 4/10, 4/10; Homer1a, 3/16, 11/16, 13/16; Homer1a W24A, 0/11, 1/11, 3/11; Homer1c, 3/11, 7/11, 10/11; Homer1c W24A, 8/16, 13/16, 15/16. (e) Analysis of each of the three types of contralateral errors after expression of Homer1a, Homer1c or Homer1cW24A. (f) The normal projection and three types of contralateral errors are schematized in a sagittal view of the brain. Axons extending into the hindbrain (gray) or into the optic tectum (black) committed pathfinding errors at choice point 5. Other axons entering the tectum (white) committed a target recognition error. * $p < 0.05$ for (a) and (b), and * $p < 0.001$ for (c-e) to controls compared by χ^2 analysis.





labeled neurons in Homer1a-VV-infected animals that aberrantly extended an axon across the tectal midline increased from 11% to 24% over 24 hours. Thus, viral expression of Homer1a significantly increased (χ^2 , $p < 0.01$) the frequency with which axons cross the tectal midline.

The greater proportion of Homer1a-VV-infected animals with axons crossing the dorsal tectal midline relative to controls (Fig. 6a and b) could arise from an increased rate of axon pathfinding errors at the midline. Alternatively, the increased error rate could arise from failure to correct aberrant axon trajectories. In 48 neurons from β -gal-VV-infected animals, we observed 3 neurons (6%) with axons projecting across the tectal midline on the first day of imaging. The following day, two of the three aberrant axons had been lost, but the labeled neurons remained alive and appeared healthy. One aberrant axon persisted at least 24 hours after the first observation. Comparable error correction was seen in uninfected controls (Fig. 6b). These data indicate that in control animals, aberrant axon projections can be corrected by loss of the errant axon. In contrast, 100% of the axons in Homer1a-VV-infected animals that had crossed the midline on the first day of imaging were maintained to the second day of imaging, and elaborated branches in the contralateral tectum. This analysis indicates that aberrant axon trajectories can be corrected in control animals (at least within the 24-hour observation period). The analysis further indicates that this correction mechanism is lost in Homer1a-VV-infected animals.

DISCUSSION

The establishment of connections within the brain requires that the axonal growth cones navigate to the target region, recognize the target, and elaborate an axon arbor. Axon guidance depends on the detection of environmental cues, the interpretation of the cues as attractive or repulsive, and the transduction of this signal to machinery governing growth cone motility. Similarly, target recognition also requires detection and response to signals to stop growing. We provide evidence that the long forms of Homer have a function in axon pathfinding and target recognition. Homer may form part of a multiple protein scaffold complex in axonal growth cones that links guidance receptors to machinery governing growth cone behaviors.

We used *in vivo* imaging of tectal cell axonal projections to determine the effect of expressing wild-type and ligand-binding mutants of Homer proteins on axon pathfinding. Homer1b/c is present in tectal cell axonal growth cones, whereas Homer1a is undetectable in young neurons during the period of axon outgrowth. Interfering with Homer function by prematurely expressing the naturally occurring truncated isoform Homer1a causes axon pathfinding errors that are not seen with expression of the ligand-binding mutant Homer1aW24A. Expression of the ligand-binding mutant of the long form of Homer, Homer1cW24A, causes the same pathfinding errors as Homer1a expression. Homer1a binds to the same effectors as the long forms of Homer and can act in a dominant negative fashion to interfere with Homer function¹⁸. Homer1cW24A can also act as a dominant negative because it can sequester endogenous Homer1b/c but cannot bind Homer ligands. This would prevent the Homer dimer from linking two ligands and reduce the efficacy of signaling from guidance receptors to intracellular effectors. Finally, errors in axon pathfinding and target recognition seen with overexpression of the long form of Homer, Homer1c, suggest that the expression level of Homer1b/c within the growth cone is critical for signal transduction governing these events.

Homer affects pathfinding at specific choice points

Interference with Homer function resulted in axon pathfinding errors at stereotyped choice points in the trajectory, consistent with studies in *Drosophila* and zebrafish, demonstrating that specific constellations of transmembrane receptors and signaling molecules govern growth cone behaviors at particular choice points^{28,29}. The location of the pathfinding error at the dorsal midline or the dorso-ventral choice point is most likely due to the relative position of the growth cone in the trajectory at the time of altered Homer expression. Young neurons, which make an error at the dorsal midline, are likely in the process of extending the axon toward the midline at the time of exogenous Homer expression. Consequently, they cannot process the inhibitory guidance information at the dorsal midline, and they cross the midline instead of avoiding it.

Axons from the more mature neurons already extended past the midline choice point by the time exogenous Homer proteins were expressed. It took about two days for the axon to reach the dorso-ventral choice point, where the errant axons grew into the contralateral tectum or hindbrain. This interpretation is further supported by the observation that some axons that had aberrantly projected to contralateral optic tectum made yet another pathfinding error at the dorsal midline and crossed into the same tectum from which their journey started. Therefore, axons require Homer function to avoid the dorsal midline either early or late in their trajectory. This observation also indicates that the midline guidance cue that Homer transduces is inhibitory¹, rather than a positive signal that maintains axons in the tract along the medial edge of the tectum. The guidance cue at the dorso-ventral choice point may be either positive, drawing growth cones to the tectum, or inhibitory, preventing the growth cone from straying off the correct trajectory¹.

Some tectal axons correctly project to the contralateral tectum after expression of Homer constructs, but then extend dorsally into the tectum. Target recognition and signals to stop growing are made by the target and detected by afferent axons in a developmentally regulated manner³⁰. Our data indicate that endogenous Homer proteins transduce target recognition and stop-growing signals.

Many molecular mechanisms cooperate to guide axons to their targets. Nevertheless, axon pathfinding errors do occur normally. Most error correction is thought to occur by cell death; however, previous studies have suggested that error correction can occur during axon pathfinding³¹. Repeated *in vivo* imaging of axonal projections allowed us to observe directly that axons do make errors in their projection pattern, and that errors can be corrected over a period of less than a day by retraction of the errant axon by an apparently healthy neuron. Furthermore, the increase in numbers of aberrant projections seen in animals expressing Homer1a partially results from a failure to correct aberrant axon projections.

Requirement for a specific level of functional Homer

Expression of both wild-type Homer1c and the ligand-binding mutant of Homer1c resulted in the same axon pathfinding and target recognition errors. This suggests that the cellular processes governed by Homer require a specific level of functional Homer protein in the growth cone. Either too little or too much functional Homer protein can interfere with signaling in the growth cone. Other instances in which loss of function and overexpression of a protein result in the same phenotype have been reported^{28,32–36}. These examples include intercellular signaling molecules, cell surface receptors and intracellular signal trans-

duction molecules, indicating that events governing axon guidance and connectivity can be finely tuned at multiple points in the biochemical cascade. The data presented here suggest that signal transduction events concerning axon guidance and target recognition depend on the spatial and temporal distribution of Homer protein within the growth cone.

Possible mechanisms of Homer function

We suggest three scenarios by which Homer may regulate axon pathfinding and target recognition. In the first scenario, Homer regulates axonal pathfinding by affecting calcium signaling in growth cones. Intracellular calcium concentration within a growth cone controls growth cone motility both *in vivo*³⁷ and *in vitro*^{7–10}. A variety of environmental cues affect the spatiotemporal distribution of intracellular calcium within growth cones^{7,10}. IP₃R-mediated calcium increases are found in growth cones, and interference with IP₃R or RyR-mediated calcium release prevents neurite extension³⁸ and alters growth cone response to guidance cues⁸. Considerable evidence suggests that Homer affects calcium signaling by linking transmembrane receptors to IP₃R or RyR¹⁸ or by regulating the efficacy of different intracellular calcium signaling pathways²⁴. The long forms of Homer proteins may regulate calcium release from intracellular stores via the IP₃R or RyR in response to guidance cues signaling through transmembrane receptors. In this scenario, expression of Homer1a or Homer1cW24A could perturb the calcium signaling events required to recognize and respond to target recognition signals, or to guidance cues at the dorsal midline or the dorso-ventral choice point. Precise regulation of signaling from transmembrane receptors to intracellular calcium stores may be lost in presence of excess Homer1c.

Alternatively, the axon pathfinding errors may arise from a change in the cell surface distribution of receptor molecules on the axonal growth cones. Disrupting either the receptor trafficking^{20–22} or clustering²⁴ function of Homer could interfere with the recognition of guidance cues in the environment, leading to pathfinding errors. A third scenario is that Homer could directly regulate actin polymerization¹⁴ by transducing signals from cell surface receptors to the actin cytoskeleton.

Scaffold proteins in the growth cone

The data presented here suggest that the long forms of Homer function in axon guidance, possibly linking cell surface proteins to intracellular components required to mediate growth cone guidance decisions. In mature neurons, Homer is a scaffold protein in postsynaptic sites. The quintessential multiprotein scaffold complex in neurons is the postsynaptic density (PSD), which includes transmembrane receptor proteins, enzymes, scaffold proteins, calcium regulatory proteins, adhesion molecules and cytoskeletal proteins^{6,39}. Within the PSD, Homer, Shank and PSD95 form a submembrane scaffold that can affect signaling through mGluRs and NMDA receptors¹⁹. A large degree of overlap exists in the protein components in the PSD scaffold complex and in the signaling machinery within the growth cone. For instance, neurotransmitter receptors, adhesion molecules, protein kinases, phosphatases and cytoskeletal regulatory proteins are just some of the components found in both the PSD and growth cone. Although this degree of overlap may seem surprising at first glance given the different functions of the growth cone and the synapse, both cellular compartments do serve to detect and respond to extracellular signals. Therefore, Homer may function both in axon guidance and at the synapse, by participating in distinct signaling pathways depending on the spatiotemporal distributions of different binding partners and downstream effectors.

METHODS

Vaccinia virus construction and infection. Vaccinia virus (VV) encoding the full length open reading frame of rat Homer1a cDNA (amino acids 1–186) was generated and used to infect *Xenopus* CNS neurons as previously described^{40,41}. All viruses also express β -galactosidase (β -gal) behind a weaker p7.5 viral promoter⁴¹. Infection with β -gal VV does not affect morphological or synaptic development of the retinotectal system⁴².

Electroporation. Tectal neurons were labeled by single-cell electroporation²⁷ with purified pEGFP (Clontech, Palo Alto, California). Alternatively, targeted electroporation was used to express genes in a single optic tectal lobe. DNA solution (75–125 nl, 0.5 μ g/ μ l in 2 mM CaCl₂, colored with fast green) was microinjected into the brain ventricle of anesthetized stage 44–45 tadpoles. Platinum electrodes (1–2 mm) were placed on the skin, on either side of the midbrain, and 3–5 pulses of 50 V with an exponential decay of $\tau = 70$ ms were delivered. Electroporation did not cause an increase in cell death (data not shown). A range of DNA concentrations from 0.2–2.0 μ g/ μ l yielded comparable levels of GFP expression. Homer constructs were either electroporated alone (GFP fusion constructs) or mixed in equal proportion with pEGFP. The constructs used were pEGFP (Clontech), Homer1a or Homer1aW24A driven by CMV promoter in the pRK5 vector, and GFP-Homer1a, GFP-Homer1c, or GFP-Homer1cW24A fusion proteins in the pEGFP vector. Plasmids were coded before electroporation. All data acquisition and analysis were done blind to treatment.

Dye labeling. Tectal neurons were labeled with either biocytin (0.5% in PBS) or DiI (0.02% 1,1'-dioctadecyl-3,3,3',3'-tetramethylindocarbocyanine perchlorate, DiI; Molecular Probes, Eugene, Oregon) in 100% ethanol, using 1 to 10 nA positive current applied in 3 to 10 pulses of 1 to 200 ms duration⁴³. Higher pulse frequency, intensity and duration were used to label clusters of neurons, whereas lower parameters were used to obtain single-cell labeling. DiI labels projection axons more efficiently than GFP. Animals labeled with biocytin were anesthetized 24 h later and fixed in 4% paraformaldehyde, and processed to visualize the biocytin as follows. Isolated brains were incubated in blocking solution (PBS, 0.3% Triton X-100, and 5% goat serum) overnight at 4°C. Brains were then incubated in FITC-tagged streptavidin (1:200, Amersham Pharmacia Biotech, Piscataway, New Jersey) overnight at 4°C, rinsed extensively in PBS and mounted in Vectashield (Vector Labs, Burlingame, California).

Image acquisition. Confocal images were collected in 2–4 μ m steps through the entire z-dimension of labeled neurons with a Noran Instruments XL laser scanning confocal attachment mounted on an upright Nikon Optiphot through a 40 \times Nikon oil immersion lens (1.30 NA). Each optical section was an average of 8–16 frames.

Two-photon images were collected on a custom-built instrument modified from an Olympus Fluoview confocal scan box mounted on an Olympus BX50WI microscope (Olympus America, Melville, New York), with a Tsunami femtosecond-pulsed Ti:Sapphire laser (Spectra Physics, Mountain View, California). We used an Olympus LUMPlanFl/IR 40 \times water immersion lens at 1–2 μ m steps through the entire z-dimension of GFP-labeled neurons. Each optical section was an average of three frames. Animals were anesthetized with 0.01% MS222 during screening and imaging, and recovered from anesthesia between imaging sessions. For DiI-labeled specimens, the first image was obtained one to three hours after labeling. Subsequent images were obtained at 24-h intervals over the next two days. For GFP-labeled specimens, the first image was obtained 24 h after labeling. Subsequent images were obtained at daily intervals over five days. GFP-filled axons could be reliably traced three days after electroporation.

Image analysis. Image stacks were analyzed in both two- and three-dimensional projections using Object Image (Norbert Vischer, University of Amsterdam, Netherlands). Montages were constructed from two-dimensional projections of confocal stacks in Adobe PhotoShop. To aid in the visualization of dorsal versus ventral localization of axonal projections, optical sections collected through the dorsal half (0–80 μ m) of the brain were pseudocolored red, whereas optical sections collected through the ventral half (80–200 μ m) of the brain were pseudocolored green.



Tectal explant cultures. Tectal lobes from anesthetized (0.05% MS222) stage 48 *Xenopus laevis* tadpoles were dissected into sterile Ca^{2+} and Mg^{2+} free HBST saline, containing 0.3 mM EDTA (5.8 mM NaCl, 0.6 mM KCl, 5.0 mM HEPES, pH 7.7). All membranes were removed, including the pia, and the lobes were cut in half. Tissue pieces were rinsed twice in fresh sterile HBST (including 0.3 mM $\text{CaCl}_2 \cdot 2\text{H}_2\text{O}$ and 0.83 mM $\text{MgSO}_4 \cdot 7\text{H}_2\text{O}$), then placed on coverslips coated in laminin (50 $\mu\text{g}/\text{ml}$). The explants were left for several hours to settle before addition of culture medium containing 50% L15, 10% fetal calf serum, 25% saline (95 mM NaCl, 1 mM KCl, 0.6 mM $\text{CaCl}_2 \cdot 2\text{H}_2\text{O}$, 3.9 $\text{MgSO}_4 \cdot 7\text{H}_2\text{O}$, 4 mM glutamine, 8.4 mM HEPES) and 5% serum (5 ng/ml sodium selenite, 5 $\mu\text{g}/\text{ml}$ transferin, 5 $\mu\text{g}/\text{ml}$ insulin, 5000U penicillin streptomycin). After four days at room temperature, cultures were processed for immunocytochemistry.

Immunostaining and western blot analysis. Tectal explant cultures were fixed in 4% paraformaldehyde, washed first in 0.1 M phosphate buffer (PB), second in PB containing 0.3% Triton X-100 (PBX; Sigma, St. Louis, Missouri); third in PBX containing 5% normal goat serum. Cultures were incubated for 2 h at room temperature in anti-Homer 1b/c antibody (1:1000 in PB containing 0.03% Triton X-100), washed in PBX and incubated for 1 h at room temperature in FITC-tagged secondary antibody. For immunostaining brain sections, stage 46–47 tadpoles were fixed in 4% paraformaldehyde in PB overnight at 4°C, rinsed, cryoprotected, and cut into 20- μm horizontal cryostat sections. Sections were preincubated with blocking solution containing 5% goat serum and 0.3% Triton X-100 in PB for 1 h followed by an overnight incubation at 4°C in anti-Homer1b/c antibodies diluted 1:1000 in blocking solution¹⁷. Sections were incubated in fluorescently tagged secondary antibody for two hours at room temperature, rinsed in PBS and mounted in Vectashield. For western blots, proteins in tissue homogenates were separated by SDS-PAGE and transferred to nitrocellulose. Blots were incubated in Tween, followed by a 1:100 dilution of the anti-Homer1a/b/c or 1:1000 of anti-Homer1b/c antibody. Blots were rinsed and incubated in 1:1000 dilution of HRP-tagged goat-anti rabbit secondary antibody. The immunoreactive bands were visualized with the ECL chemiluminescence kit.

ACKNOWLEDGEMENTS

We thank K. Bronson, N. Dawkins and B. Burbach for technical help, E. Ruthazer, P. O'Brien, B. Burbach and K. Svoboda for building the two-photon microscope, E. Ruthazer for help with the two-photon image acquisition and analysis, J.C. Tu and B. Xiao for constructs, and members of the Cline lab for discussions. A. Demetriades helped with experiments through the Undergraduate Research Program at CSHL. Supported by the NIH (H.T.C., K.H. and P.W.), the Eppley Foundation (H.T.C.) and the Helen Hoffritz Fund (H.T.C.).

RECEIVED 8 DECEMBER 2000; ACCEPTED 19 MARCH 2001

- Goodman, C. S. Mechanisms and molecules that control growth cone guidance. *Annu. Rev. Neurosci.* **19**, 341–377 (1996).
- Hu, S. & Reichardt, L. F. From membrane to cytoskeleton: enabling a connection. *Neuron* **22**, 419–422 (1999).
- Lin, C. H., Thompson, C. A. & Forscher, P. Cytoskeletal reorganization underlying growth cone motility. *Curr. Opin. Neurobiol.* **4**, 640–647 (1994).
- Fraser, I. D. & Scott, J. D. Modulation of ion channels: a "current" view of AKAPs. *Neuron* **23**, 423–426 (1999).
- Klauck, T. M. *et al.* Coordination of three signaling enzymes by AKAP79, a mammalian scaffold protein. *Science* **271**, 1589–1592 (1996).
- Sheng, M. & Pak, D. T. Glutamate receptor anchoring proteins and the molecular organization of excitatory synapses. *Ann. NY Acad. Sci.* **868**, 483–493 (1999).
- Kater, S. B. & Mills, L. R. Regulation of growth cone behavior by calcium. *J. Neurosci.* **11**, 891–899 (1991).
- Hong, K., Nishiyama, M., Henley, J., Tessier-Lavigne, M. & Poo, M.-m. Calcium signalling in the guidance of nerve growth by netrin-1. *Nature* **403**, 93–98 (2000).
- Zheng, J. Q. Turning of nerve growth cones induced by localized increases in intracellular calcium ions. *Nature* **403**, 89–93 (2000).
- Zheng, J. Q., Poo, M.-m. & Connor, J. A. Calcium and chemotropic turning of nerve growth cones. *Perspect. Dev. Neurobiol.* **4**, 205–213 (1996).
- Bentley, D. & O'Connor, T. P. Cytoskeletal events in growth cone steering. *Curr. Opin. Neurobiol.* **4**, 43–48 (1994).

- Brakeman, P. R. *et al.* Homer: a protein that selectively binds metabotropic glutamate receptors. *Nature* **386**, 284–288 (1997).
- Kato, A., Ozawa, F., Saitoh, Y., Hirai, K. & Inokuchi, K. vesl, a gene encoding VASP/Ena family related protein, is upregulated during seizure, long-term potentiation and synaptogenesis. *FEBS Lett.* **412**, 183–189 (1997).
- Nedivi, E., Fieldust, S., Theill, L. & Hevroni, D. A set of genes expressed in response to light in the adult cerebral cortex and regulated during development. *Proc. Natl. Acad. Sci. USA* **93**, 2048–2053 (1996).
- Tadokoro, S., Tachibana, T., Imanaka, T., Nishida, W. & Sobue, K. Involvement of unique leucine-zipper motif of PSD-Zip45 (Homer 1c/vesl-1L) in group I metabotropic glutamate receptor clustering. *Proc. Natl. Acad. Sci. USA* **96**, 13801–13806 (1999).
- Shiraishi, Y. *et al.* Cupidin, an isoform of Homer/Vesl, interacts with the actin cytoskeleton and activated rho family small GTPases and is expressed in developing mouse cerebellar granule cells. *J. Neurosci.* **19**, 8389–8400 (1999).
- Xiao, B. *et al.* Homer regulates the association of group I metabotropic glutamate receptors with multivalent complexes of homer-related, synaptic proteins. *Neuron* **21**, 707–716 (1998).
- Tu, J. C. *et al.* Homer binds a novel proline-rich motif and links group I metabotropic glutamate receptors with IP3 receptors. *Neuron* **21**, 717–726 (1998).
- Tu, J. C. *et al.* Coupling of mGluR/Homer and PSD-95 complexes by the Shank family of postsynaptic density proteins. *Neuron* **23**, 583–592 (1999).
- Ciruela, F., Soloviev, M. M., Chan, W.-Y. & McIlhinney, R. A. J. Homer-1c/vesl-1L modulates the cell surface targeting of metabotropic glutamate receptor type 1a: Evidence for an anchoring function. *Mol. Cell. Neurosci.* **15**, 36–50 (2000).
- Ciruela, F., Soloviev, M. M. & McIlhinney, R. A. Co-expression of metabotropic glutamate receptor type Ialpha with homer-1a/Vesl-1S increases the cell surface expression of the receptor. *Biochem. J.* **353**, 795–803 (1999).
- Roche, K. W. *et al.* Homer 1b regulates the trafficking of group I metabotropic glutamate receptors. *J. Biol. Chem.* **274**, 25953–25957 (1999).
- Kato, A. *et al.* Novel members of the Vesl/Homer family of PDZ proteins that bind metabotropic glutamate receptors. *J. Biol. Chem.* **273**, 23969–23975 (1998).
- Kammermeier, P. J., Xiao, B., Tu, J. C., Worley, P. F. & Ikeda, S. R. Homer proteins regulate coupling of group I metabotropic glutamate receptors to N-type calcium and M-type potassium channels. *J. Neurosci.* **20**, 7238–7245 (2000).
- Beneken, J. *et al.* Structure of the Homer EVH1 domain-peptide complex reveals a new twist in polyproline recognition. *Neuron* **26**, 143–154 (2000).
- Wu, G.-Y., Zou, D. J., Rajan, I. & Cline, H. T. Dendritic dynamics in vivo change during neuronal maturation. *J. Neurosci.* **19**, 4472–4483 (1999).
- Haas, H., Sin, W.-C., Javaherian, A., Li, Z. & Cline, H. T. Single-cell electroporation for in vivo neuronal gene expression. *Neuron* **29**, 571–581 (2001).
- Luo, L., Jan, L. & Jan, Y. N. Small GTPases in axon outgrowth. *Perspect. Dev. Neurobiol.* **4**, 199–204 (1996).
- Karlstrom, R. O., Trowe, T. & Bonhoeffer, F. Genetic analysis of axon guidance and mapping in the zebrafish. *Trends Neurosci.* **20**, 3–8 (1997).
- Zhang, Q. & Mason, C. A. Developmental regulation of mossy fiber afferent interactions with target granule cells. *Dev. Biol.* **195**, 75–87 (1998).
- Rajan, I. & Denburg, J. L. Error correction during guidance of pioneer axons in the leg of the cockroach embryo. *Roux's Arch. Dev. Biol.* **205**, 476–485 (1996).
- Gao, F.-B., Kahwi, M., Brenman, J. E., Jan, L. Y. & Jan, Y. N. Control of dendritic field formation in *Drosophila*: the roles of Flamingo and competition between homologous neurons. *Neuron* **28**, 91–101 (2000).
- Krasnow, R. E., Wong, L. L. & Adler, P. N. Dishevelled is a component of the frizzled signaling pathway in *Drosophila*. *Development* **121**, 4095–4102 (1995).
- Krasnow, R. E. & Adler, P. N. A single frizzled protein has a dual function in tissue polarity. *Development* **120**, 1883–1893 (1994).
- Cabelli, R. J., Shelton, D. L., Segal, R. A. & Shatz, C. J. Blockade of endogenous ligands of trkB inhibits formation of ocular dominance columns. *Neuron* **19**, 63–76 (1997).
- Cabelli, R. J., Hohn, A. & Shatz, C. J. Inhibition of ocular dominance column formation by infusion of NT-4/5 or BDNF. *Science* **267**, 1662–1666 (1995).
- Gomez, T. M. & Spitzer, N. C. In vivo regulation of axon extension and pathfinding by growth-cone calcium transients. *Nature* **397**, 350–355 (1999).
- Takei, K., Shin, R. M., Inoue, T., Kato, K. & Mikoshiba, K. Regulation of nerve growth mediated by inositol 1,4,5-trisphosphate receptors in growth cones. *Science* **282**, 1705–1708 (1998).
- Kennedy, M. B. Signal transduction molecules at the glutamatergic postsynaptic membrane. *Brain Res. Brain Res. Rev.* **26**, 243–257 (1998).
- Mockett, M., Smith, G. L. & Moss, B. in *DNA Cloning: A Practical Approach* (ed. Glover, D. M.) 191–210 (IRL, Oxford, 1985).
- Wu, G.-Y., Zou, D.-J., Koothian, T. & Cline, H. T. Infection of frog neurons with Vaccinia Virus permits in vivo expression of foreign proteins. *Neuron* **14**, 681–684 (1995).
- Cline, H. T. Dendritic arbor development and synaptogenesis. *Curr. Opin. Neurobiol.* **11**, 118–126 (2001).
- Cline, H. T., Edwards, J. A., Rajan, I., Wu, G. Y. & Zou, D. J. in *Imaging: A Laboratory Manual* (eds. Yuste, R., Lanni, F. & Konnerth, A.) 13.1–13.12 (Cold Spring Harbor Laboratory Press, Cold Spring Harbor, 1999).